Electronic Supplementary Material (ESI) for Dalton Transactions.

Supporting Information

Stable Fe(III) phenoxyimines as selective and robust CO_2/epoxide coupling catalysts

Eszter Fazekas,[a] Gary S. Nichol,[a] Michael P. Shaver[a] and Jennifer A. Garden*[a]

[a]EaStCHEM School of Chemistry, University of Edinburgh, Edinburgh, EH9 3FJ, UK.

Table of contents

1. ^{1}H and ^{13}C NMR spectra of ligands L1-L3

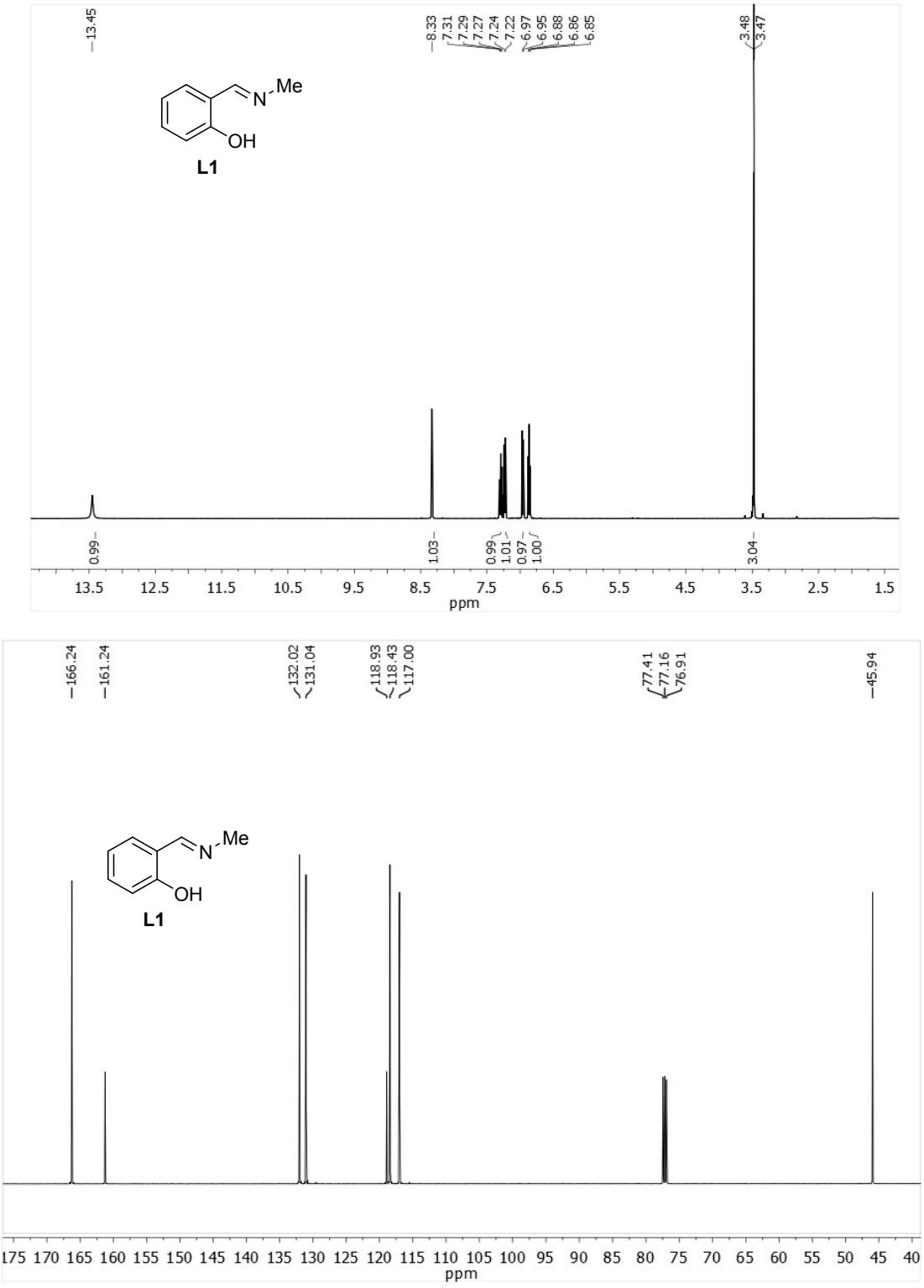

Figure S1 ^{1}H and ^{13}C NMR spectra of **L1** in $CDCl_3$ at 20°C.

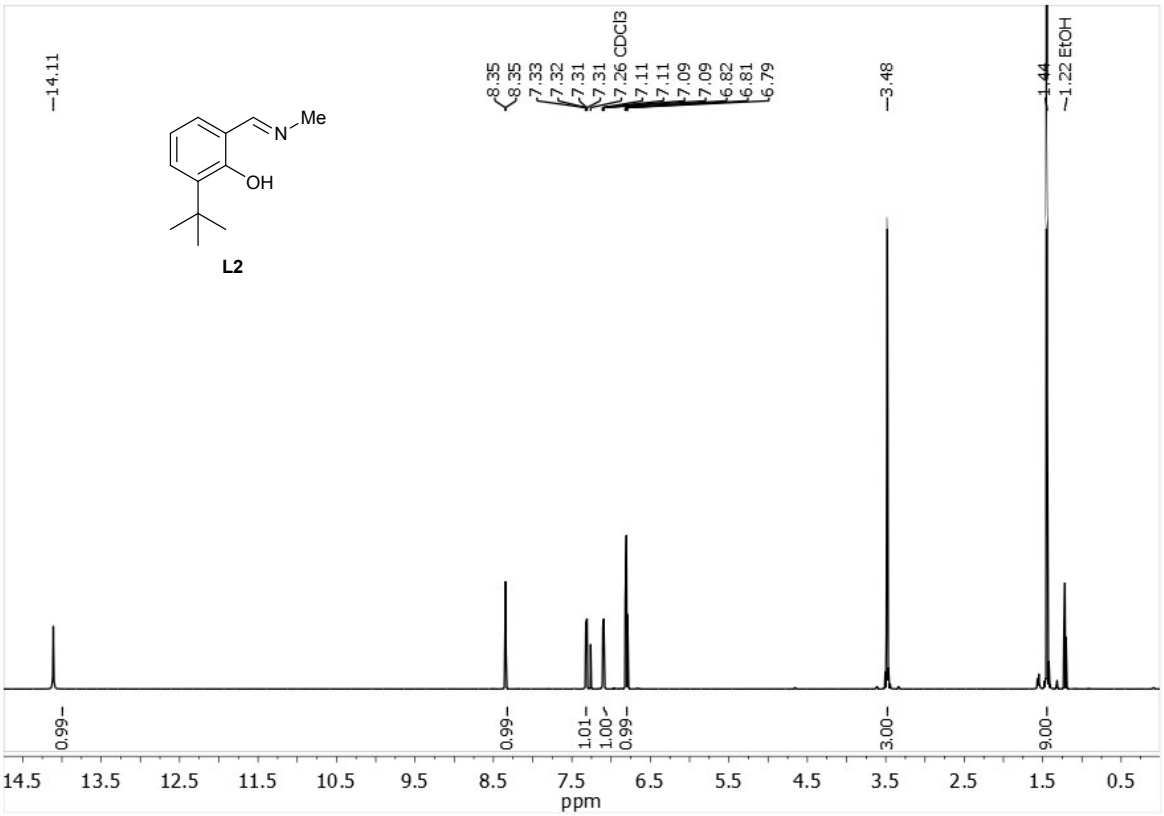

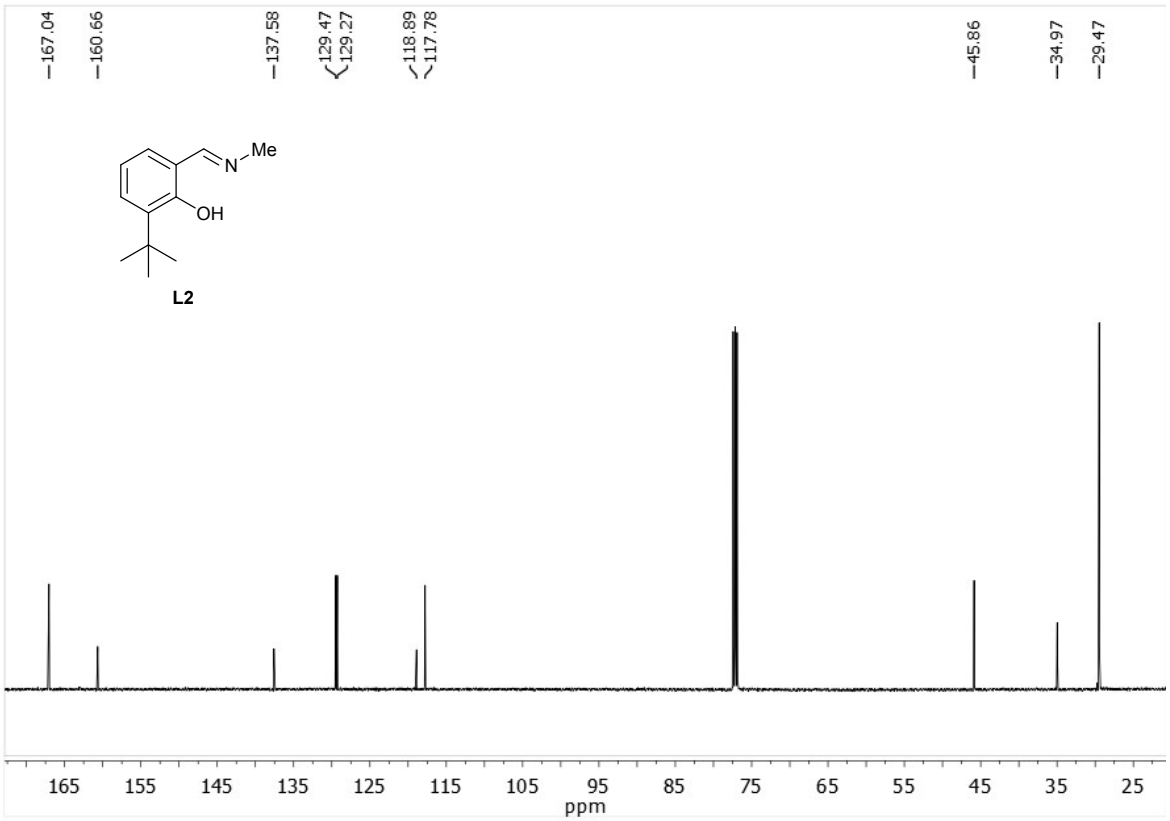

Figure S2 ^{1}H and ^{13}C NMR spectra of **L2** in $CDCl_3$ at 20°C.

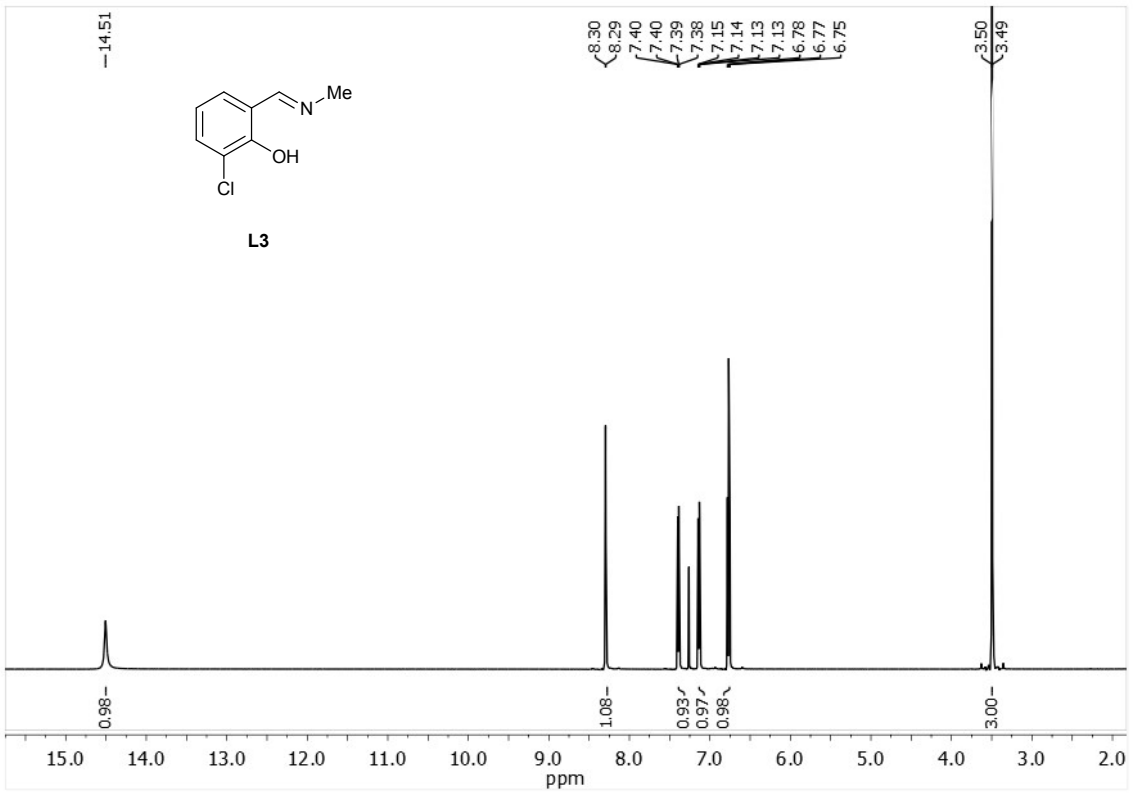

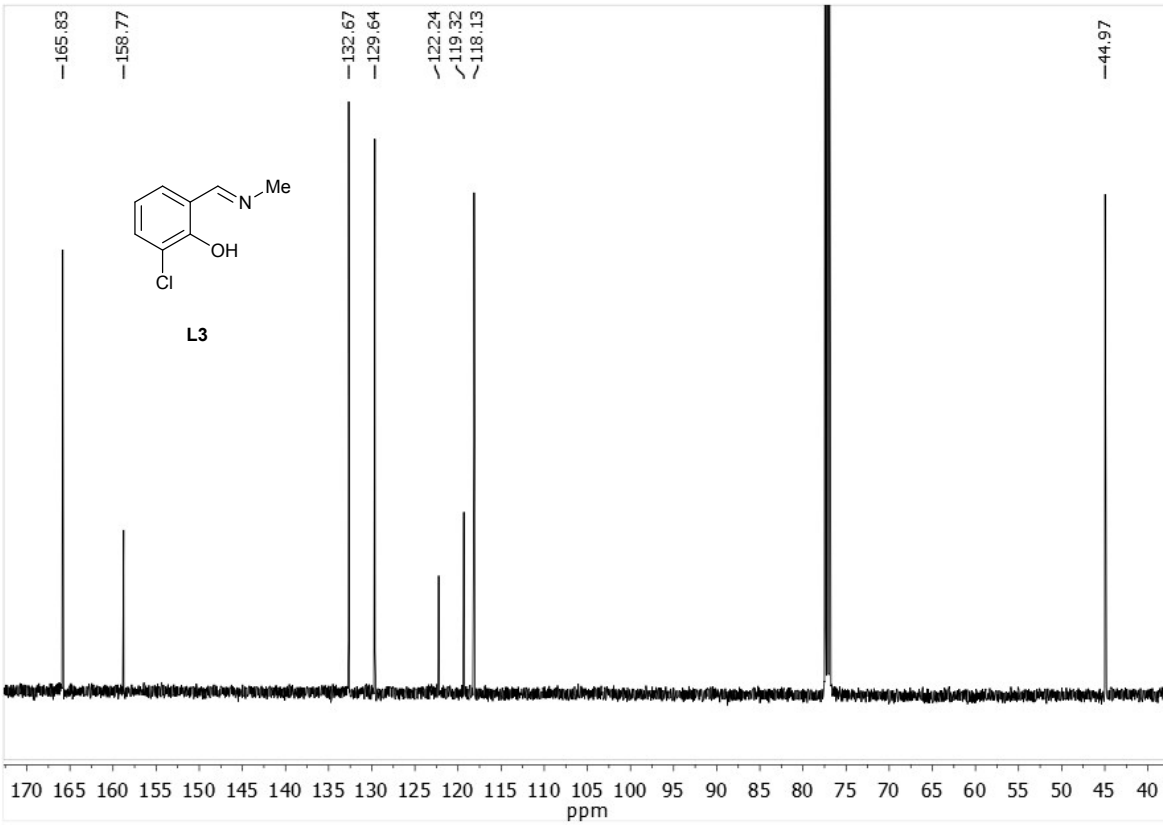

Figure S3 ^{1}H and ^{13}C NMR spectra of **L3** in $CDCl_3$ at 20°C.

2. HRMS spectra of complexes C1-C3

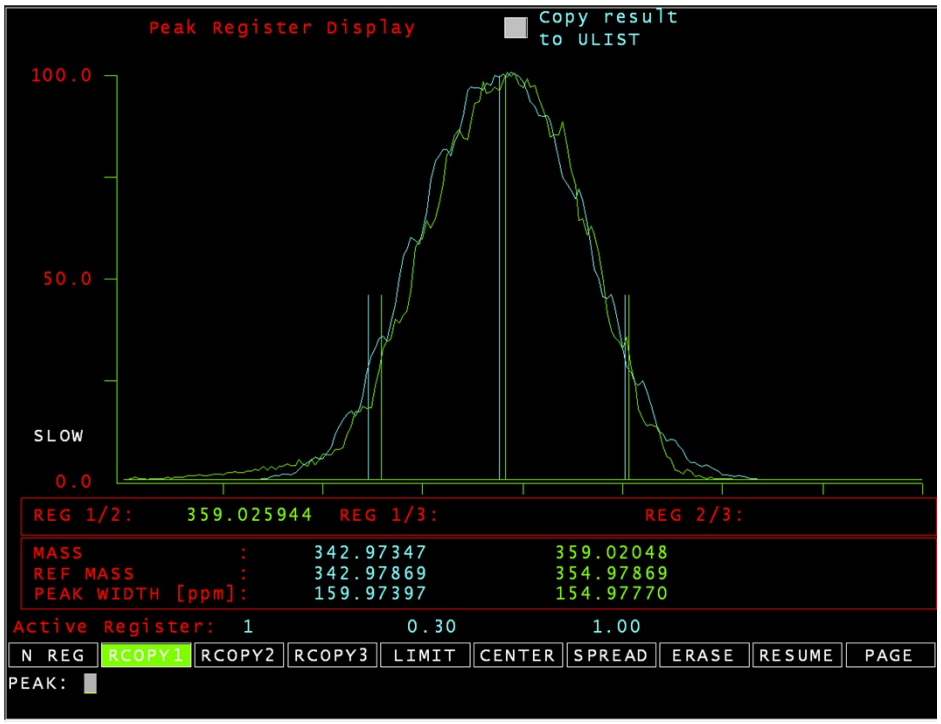

Figure S4 HRMS peak of **C1**.

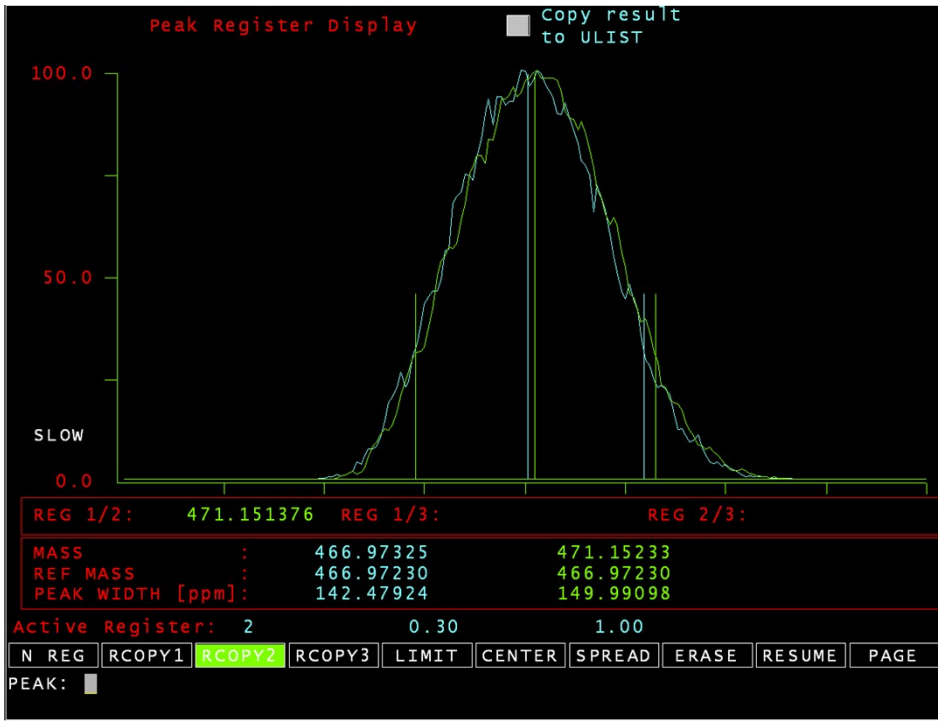

Figure S5 HRMS peak of **C2**.

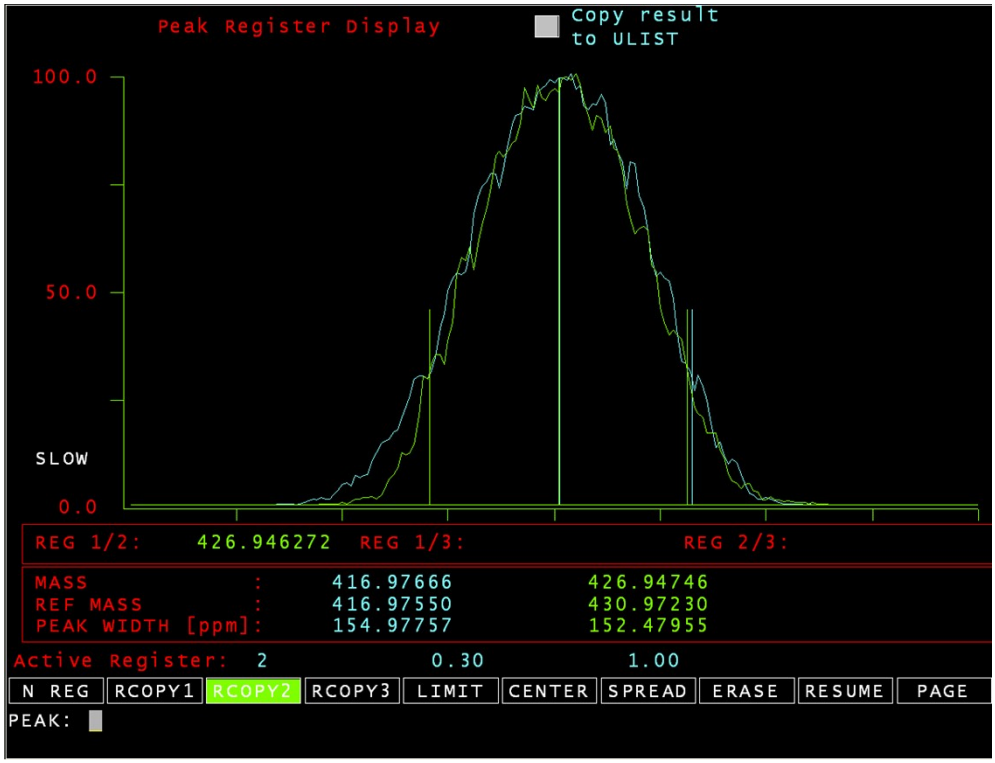

Figure S6 HRMS peak of **C3**.

3. ^{1}H NMR spectra of crude CO_2/epoxide coupling reaction mixtures

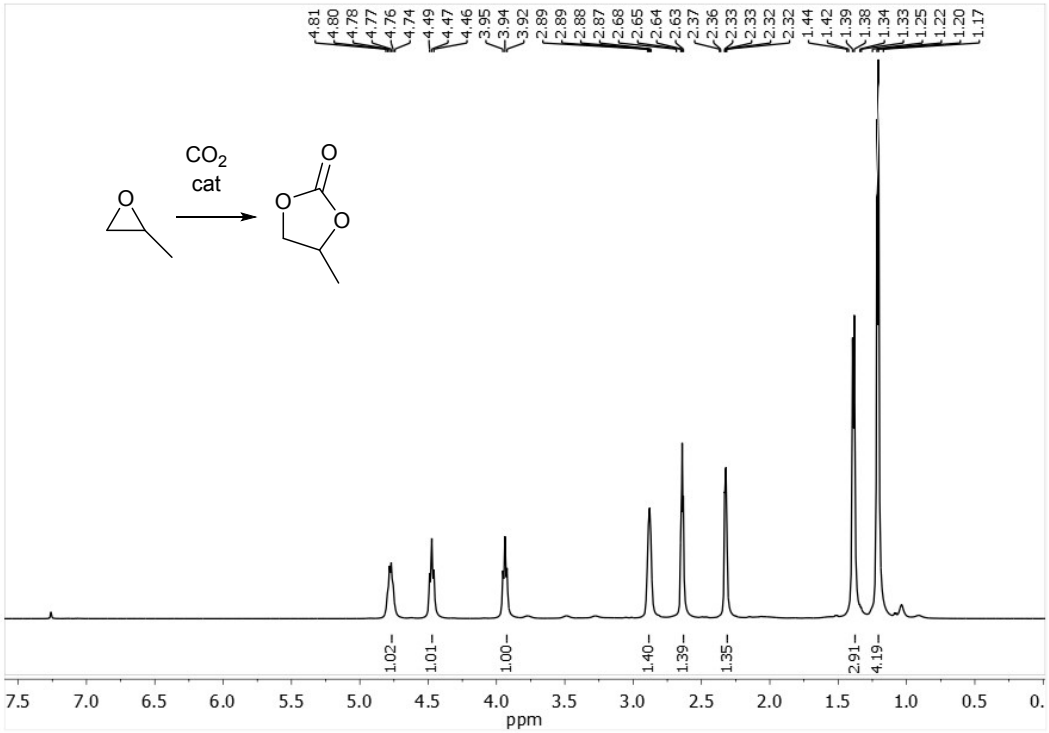

Figure S7 Typical ^{1}H NMR spectrum of a CO_2/propylene oxide coupling crude reaction mixture in $CDCl_3$ at 20°C. Conversion was determined *via* integration of the CH_3 propylene carbonate (product) peak at 1.37 ppm against the CH_3 propylene oxide (starting material) peak at 1.20 ppm.

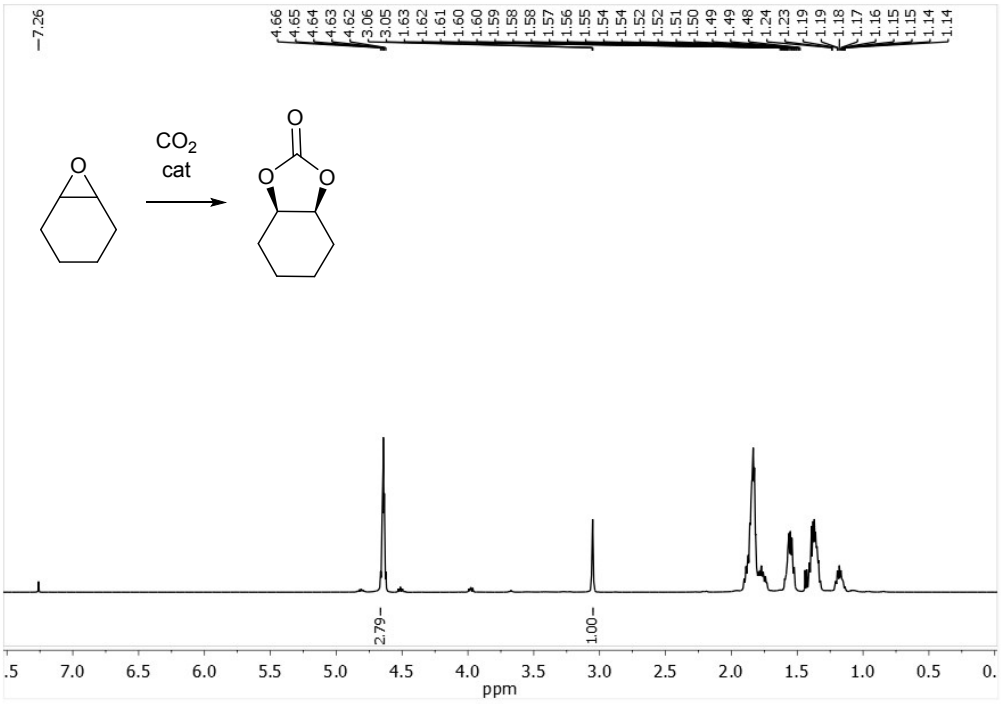

Figure S8 Typical ^{1}H NMR spectrum of a CO_2/cyclohexene oxide coupling crude reaction mixture in $CDCl_3$ at 20°C. Conversion was determined *via* integration of the OC*H*CH_2CH_2 cyclohexene carbonate (product) peak at 4.66 ppm against the OC*H*CH_2CH_2 cyclohexene oxide (starting material) peak at 3.09 ppm.[1]

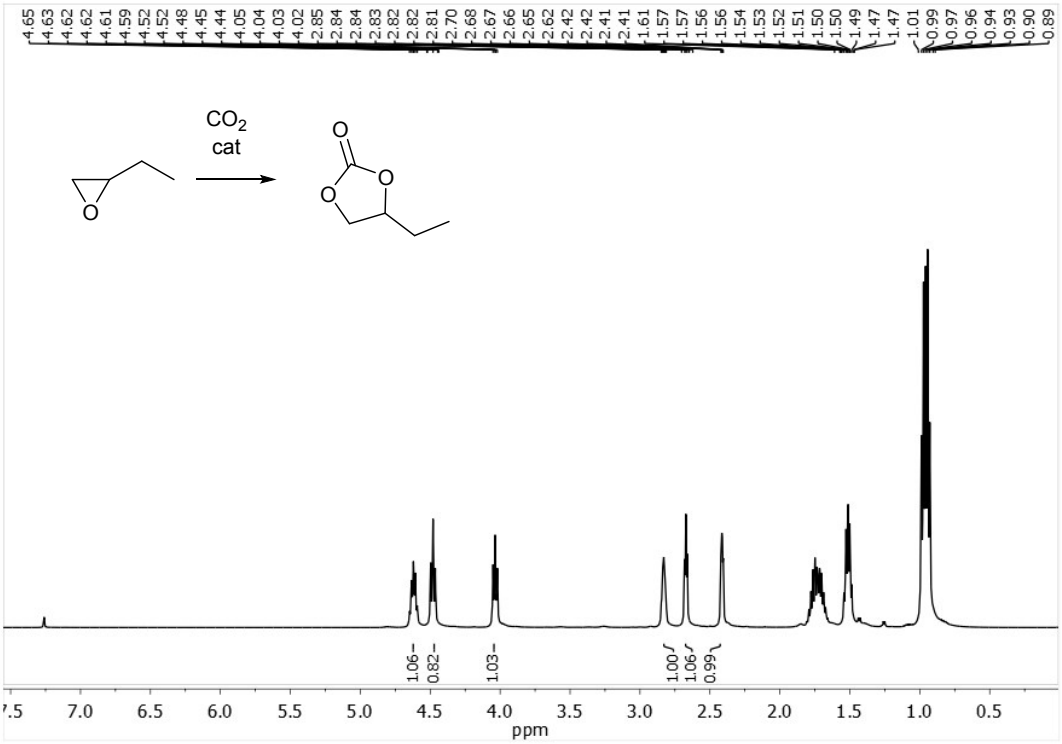

Figure S9 Typical ^{1}H NMR spectrum of a CO_2/1,2-epoxybutane coupling crude reaction mixture in $CDCl_3$ at 20°C. Conversion was determined *via* integration of the OC*H* butylene carbonate (product) peak at 4.63 ppm against the OC*H*CH_2CH_2 1,2-epoxybutane (starting material) peak at 2.83 ppm.

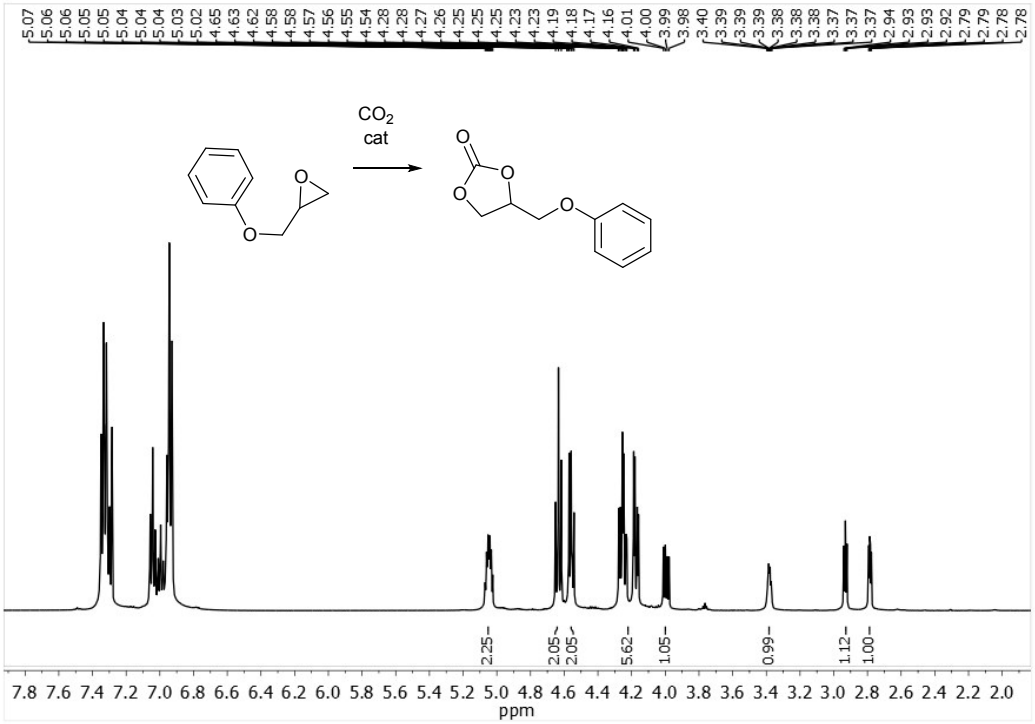

Figure S10 Typical ^{1}H NMR spectrum of a CO_2/1,2-epoxy-3-phenoxypropane coupling crude reaction mixture in $CDCl_3$ at 20°C. Conversion was determined *via* integration of the OC*H* carbonate (product) peak at 4.25 ppm against the OC*H*C 1,2-epoxy-3-phenoxypropane (starting material) peak at 3.39 ppm.

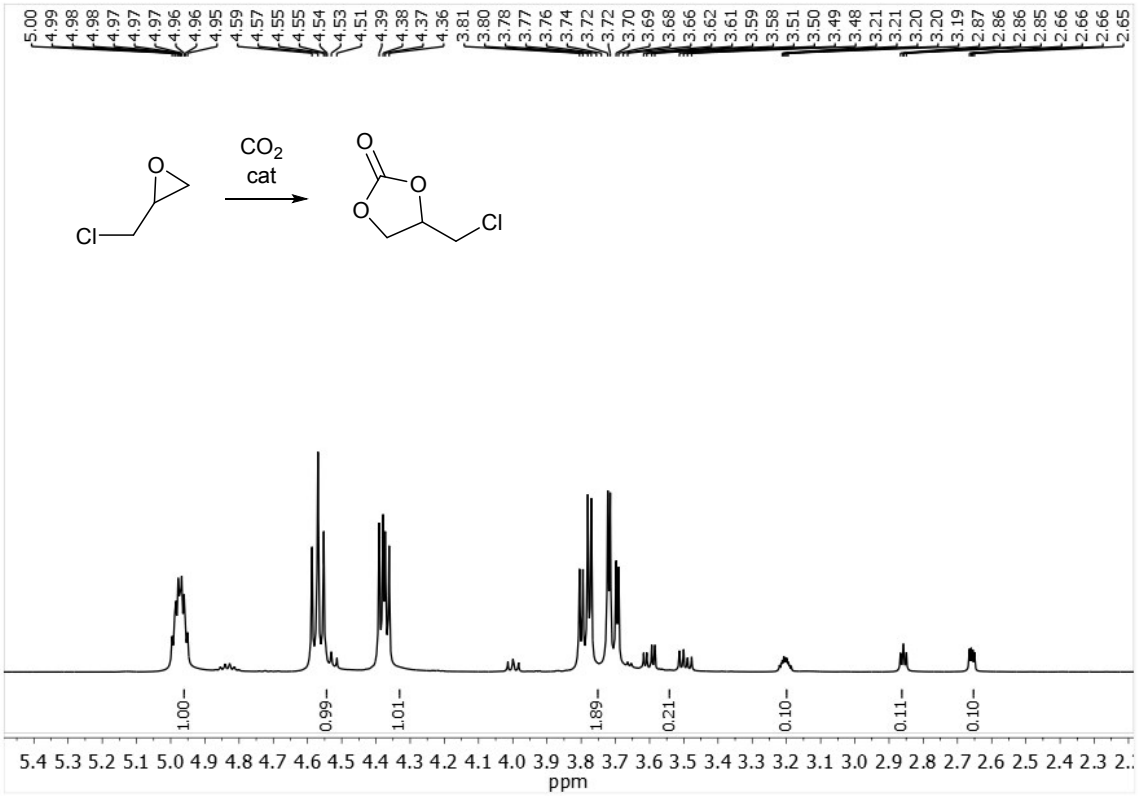

Figure S11 Typical ^{1}H NMR spectrum of a CO_2/epichlorohydrin coupling crude reaction mixture in $CDCl_3$ at 20°C. Conversion was determined *via* integration of the OC*H* carbonate (product) peak at 4.98 ppm against the OC*H* epichlorohydrin (starting material) peak at 3.21 ppm.[2]

4. Kinetic plot of CO_2/propylene oxide coupling reaction (0.01 mol% catalyst loading)

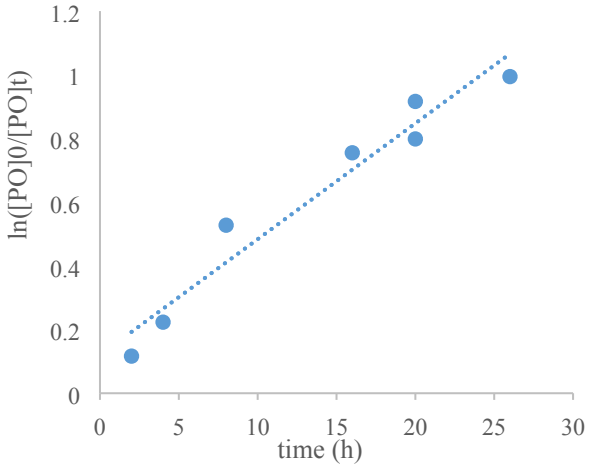

Figure S12 Kinetic plot for the synthesis of propylene carbonate using **C3** with 10000 equivalents of substrate. Conditions: 100 ml stainless steel autoclaves, 20 bar CO_2 pressure, 120°C, neat. Conversion was determined using ^{1}H NMR spectra of crude reaction mixtures.

5. Data for CO_2/cyclohexene oxide coupling reactions

Table S1 Synthesis of cyclohexene carbonate from CO_2 and cyclohexene oxide catalysed by complex **C3**.

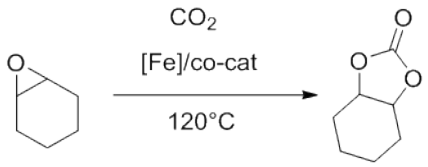

Entry	Complex	t (h)	[CHO]/[Fe]	Co-catalyst	[Co-cat] /[Fe]	Conv. (%)	TON	TOF (h^{-1})
1	**C3**	2	2000	TBABr	2	8	160	80
2	**C3**	24	2000	TBABr	2	56	1120	47
3	**C3**	48	2000	TBABr	2	74	1480	31

Conditions: 100 ml stainless steel autoclaves, 20 bar CO_2 pressure, 120°C, neat. Conversion was determined using ^{1}H NMR spectra of crude reaction mixtures.

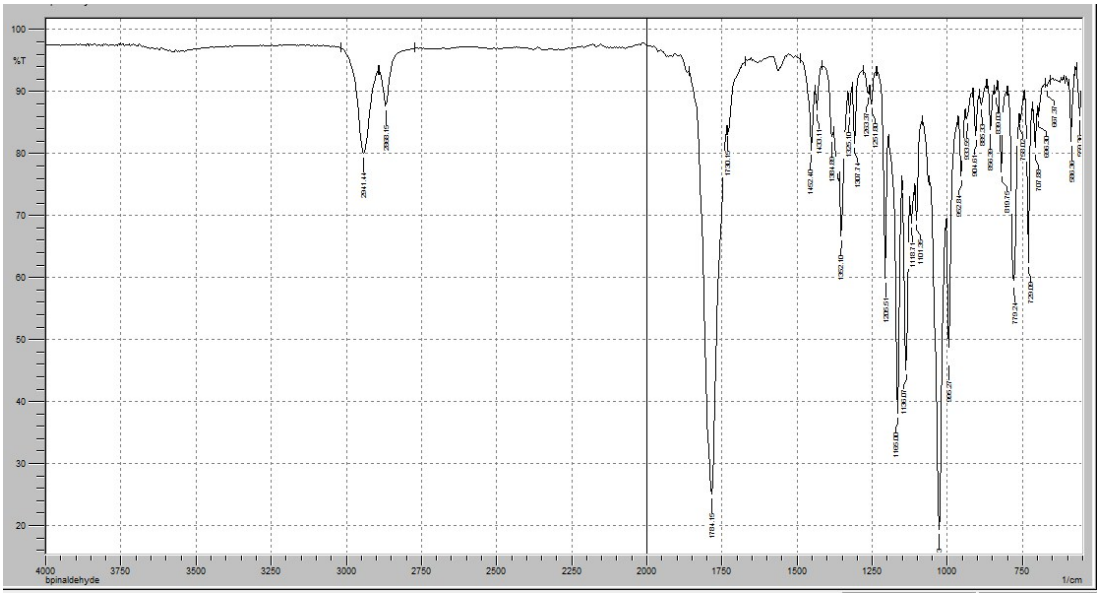

Figure S13 IR spectrum of a crude CO_2/cyclohexene oxide coupling reaction mixture. The absence of peaks in the 1014 cm^{-1}, 1239-1176 cm^{-1}, and 1731-1787 cm^{-1} bands indicates no polymer formation.[3]

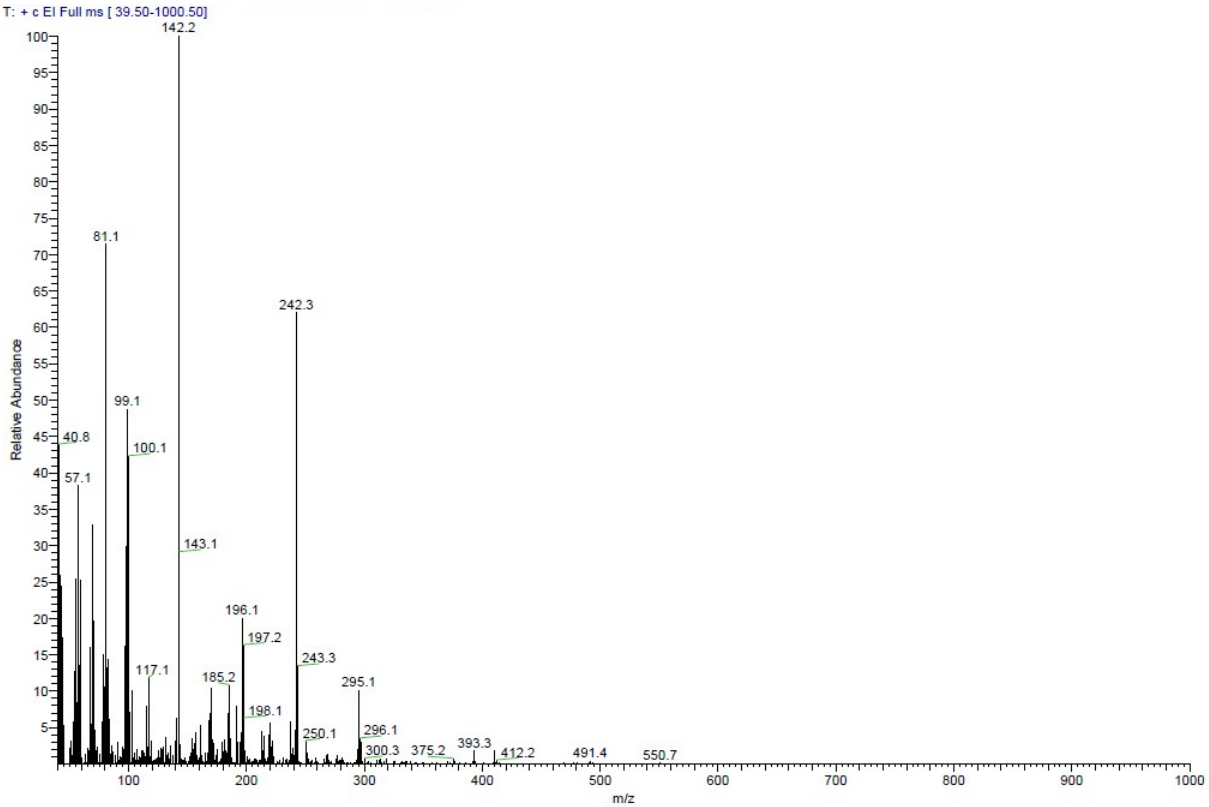

Figure S14 EI mass spectrum of a crude CO_2/cyclohexene oxide coupling reaction mixture. The absence of peaks above 550 m/z value indicates no polymer formation.

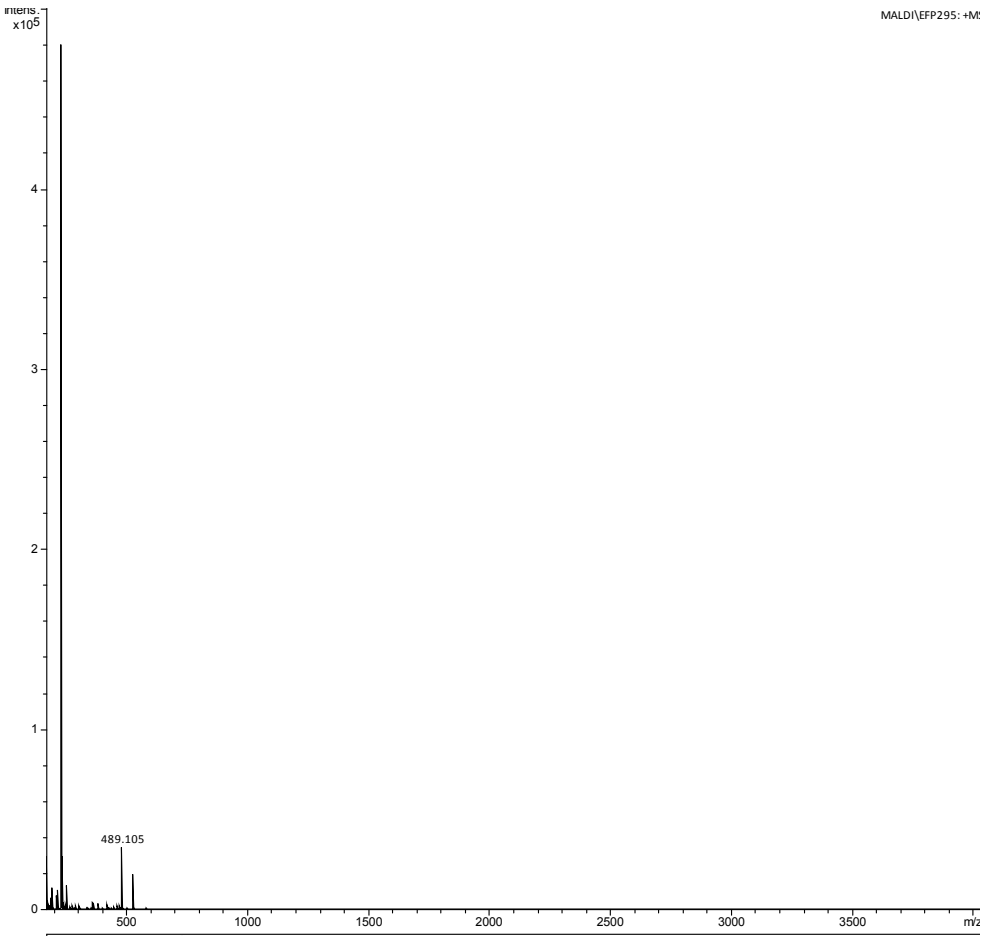

Figure S15 MALDI spectrum of a crude CO_2/cyclohexene oxide coupling reaction mixture. The absence of peaks above 538 m/z value indicates no polymer formation.

6. Comparison with other Fe complexes for CO_2/epoxide coupling in the literature

Table S2 Selected literature data for the synthesis of propylene carbonate and cyclohexene carbonate.

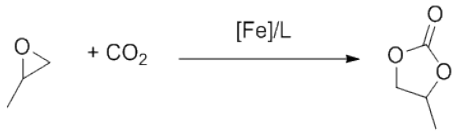

Entry	Fe/co-cat/PO	T (°C)	p (bar)	t (h)	Conv. (%)	TON	TOF (h^{-1})
1[a]	1/2/2000	120	20	1	44	880	880
2[4]	1/5/1000	35	1	1	10	100	100
3[5]	1/10/10000	120	20	1	52	5200	5200
4[6]	1/4/4000	100	20	6	27	1080	180
5[7]	1/1/100	100	15	1	100	100	100
6[8]	1/4/4000	100	20	6	87	3160	580
7[9]	1/5/100	25	10	18	88	88	5
8[10]	1/10/200	25	2	18	74	148	8
9[11]	1/0/200	80	35	20	69	690	34.5
10[11]	1/0/200	80	35	20	92	184	9
11[12]	1/1/1000	100	40	2	91	910	455

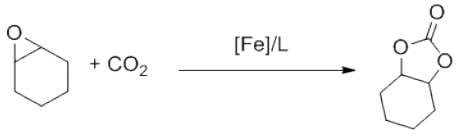

Entry	Fe/co-cat/CHO	T (°C)	p (bar)	t (h)	Conv. (%)	TON	TOF (h^{-1})
12[1]	1/0/10000	80	10	24	25	2570	107
13[13]	1/10/200	85	80	3	94	188	62

[a]Conditions: 100 ml stainless steel autoclaves, 20 bar CO_2 pressure, 120°C, neat. Conversion was determined using ^{1}H NMR spectra of crude reaction mixtures.

7. Lower temperature CO_2/propylene oxide coupling experiments

Table S3 Synthesis of propylene carbonate catalysed by complex **C3** at 100°C.

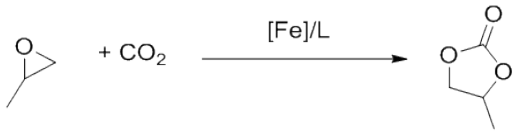

Entry	Fe/co-cat/PO	co-cat	T (°C)	p (bar)	t (h)	Conv. (%)	TON	TOF (h^{-1})	TOF/[Fe] (h^{-1})
1[8]	1/4/4000	TBABr	100	20	6	87	3480	580	290
2	1/4/4000	TBAI	100	20	6	34	1360	227	227
3	1/4/4000	TBABr	100	20	6	47	1880	313	313

Conditions: 100 ml stainless steel autoclaves, 20 bar CO_2 pressure, 100°C, neat. Conversion was determined using ^{1}H NMR spectra of crude reaction mixtures.

8. Kinetic data for the synthesis of propylene carbonate catalysed by C3.

Table S4 Synthesis of propylene carbonate catalysed by complex **C3** with 2000 and 10000 equivalents of substrate.

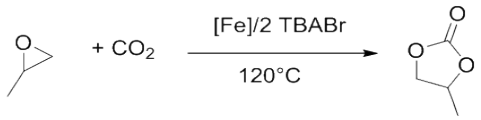

Entry	t (h)	[PO]/[Fe]	Conv. (%)	TON	TOF (h^{-1})
1	1	2000	44	880	880
2	2	2000	51	1020	510
3	3	2000	64	1280	427
4	4.5	2000	74	1480	329
5	6	2000	85	1700	283
6	2	10000	11	1100	550
7	4	10000	20	2000	500
8	8	10000	41	4100	513
9	16	10000	53	5300	331
10	20	10000	55	5500	275
11	26	10000	63	6300	242

Conditions: 100 ml stainless steel autoclaves, 20 bar CO_2 pressure, 120°C, neat. Conversion was determined using ^{1}H NMR spectra of crude reaction mixtures.

9. Catalyst decomposition studies *via* FT-IR spectroscopy

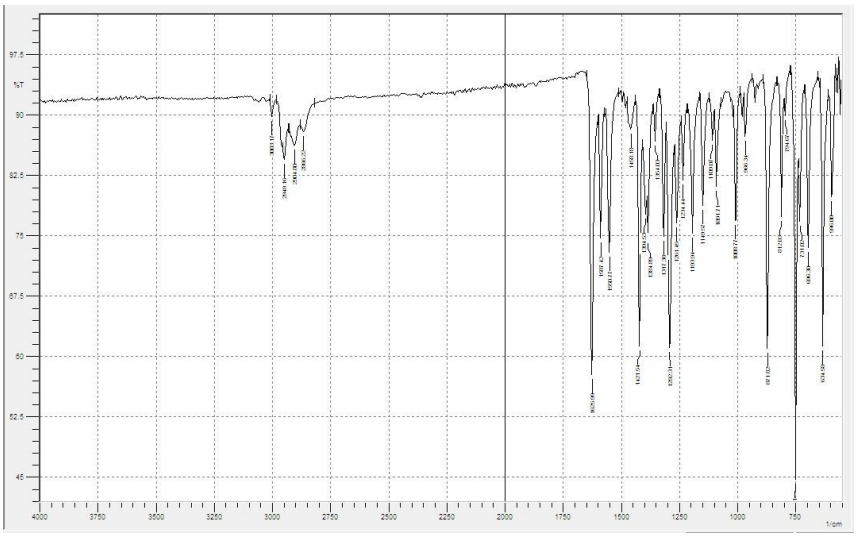

Figure S16 FT-IR spectrum of **C3** catalyst complex.

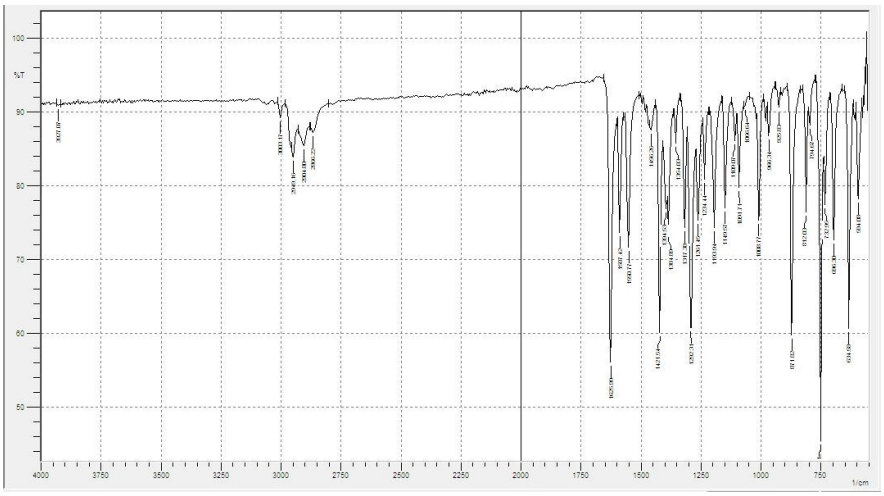

Figure S17 FT-IR spectrum of **C3** after stirring in water for 1 hour at ambient temperature, with subsequent removal of the water under vacuum. No new -OH resonance was observed, and the resonances from **C3** remain consistent between the two spectra.

10. X-ray data for Complexes C1 – C3

C1

$C_{16}H_{16}ClFeN_2O_2$, M = 359.61, T = 120 K, monoclinic, space group $I2/a$, a =12.5989(3), b = 7.39494(17), c = 17.7897(5) Å, β = 108.536(3)°, V = 1571.44(7) Å^3, Z = 4, 19409 measured reflections, 2808 (R_{int} = 0.0288) unique, final R_1 = 0.0298 (all data).

The average of the equatorial angles [Cl1-Fe1-O1, 119.50°; Cl1-Fe1-O1', 119.50°; O1-Fe1-O1', 121.00° is 120.00°, which corresponds to 100% equatorial trigonal bipyramidal character (TBP_e).[14] Defined by apical-to-equatorial bonds [N1-Fe1-O1, 90.28°; N1-Fe1-O1', 88.46°; N1-Fe1-Cl1, 91.28°], the axial trigonal bipyramidal character (TBP_a) is also high at 99.97%.

C2

$C_{55}H_{72}Cl_2Fe_2N_4O_4$, M = 1035.80, T = 120 K, monoclinic, space group $P2_1/c$, *a* = 10.8856(3), *b* = 24.3385(7), *c* = 19.8618(7) Å, β = 91.003(3)°, *V* = 5261.3(3) Å^3, *Z* = 4, 12233 measured reflections, 10913 [R_{int} = 0.1307] unique reflections, final R_1 = 0.1281 (all data).

The average of the equatorial angles [Cl1-Fe1-O1, 116.07°; Cl1-Fe1-O2, 119.34°; O1-Fe1-O1', 124.60° is 120.00°, which corresponds to 100% equatorial trigonal bipyramidal character (TBP_e).[14] Defined by apical-to-equatorial bonds [N1-Fe1-O1, 87.50°; N1-Fe1-O2, 87.60°; N1-Fe1-Cl1, 93.55°], the axial trigonal bipyramidal character (TBP_a) is also high at 97.69%.

C3

$C_{16}H_{14}Cl_3FeN_2O_2$, *M* = 428.49, T = 120 K, monoclinic, space group *C*2/*c*, *a* = 23.1547(3), *b* = 12.00241(14), *c* = 12.99462(16) Å, β = 102.4166(12)°, *V* = 3526.89(7) Å^3, *Z* = 8, 27812 measured reflections, 3677 [R_{int} = 0.0700] unique, final R_1 = 0.0431 (all data).

The average of the equatorial angles [Cl1-Fe1-O1, 117.12°; Cl1-Fe1-O2, 121.11°; O1-Fe1-O2, 121.78° is 120.00°, which corresponds to 99.97% equatorial trigonal bipyramidal character (TBP_e).[14] Defined by apical-to-equatorial bonds [N1-Fe1-O2, 89.00°; N1-Fe1-O1, 88.64°; N1-Fe1-Cl1, 92.25°], the axial trigonal bipyramidal character (TBP_a) is also high at 99.79%.

Table S2 Crystallographic data and refinement details for **C1**, **C2** and **C3** (CCDC reference numbers 1855808-1855810).

Identification code	**C1**	**C2**	**C3**
Empirical formula	$C_{16}H_{16}ClFeN_2O_2$	$C_{55}H_{72}Cl_2Fe_2N_4O_4$	$C_{16}H_{14}Cl_3FeN_2O_2$
Formula weight	359.61	1035.80	428.49
Temperature/K	120.00	120.00	120.00
Crystal system	monoclinic	monoclinic	monoclinic
Space group	I2/a	$P2_1/c$	C2/c
a/Å	12.5989(3)	10.8856(3)	23.1547(3)
b/Å	7.39494(17)	24.3385(7)	12.00241(14)
c/Å	17.7897(5)	19.8618(7)	12.99462(16)
α/°	90	90	90
β/°	108.536(3)	91.003(3)	102.4166(12)
γ/°	90	90	90
Volume/Å^3	1571.44(7)	5261.3(3)	3526.89(7)
Z	4	4	8
ρ_{calc}g/cm^3	1.520	1.3075	1.614
μ/mm^{-1}	1.137	5.730	11.142
F(000)	740.0	2191.2	1736.0
Crystal size/mm^3	0.377 × 0.295 × 0.217	0.458 × 0.170 × 0.017	0.092 × 0.075 × 0.05
Radiation	MoKα (λ = 0.71073)	Cu Kα (λ = 1.54184)	CuKα (λ = 1.54184)
2Θ range for data collection/°	6.016 to 65.776	7.26 to 152.04	7.82 to 152.05
Reflections collected	19409	12233	27812
Independent reflections	2808 [R_{int} = 0.0288, R_{sigma} = 0.0191]	10913 [R_{int} = 0.1307, R_{sigma} = 0.1073]	3677 [R_{int} = 0.0700, R_{sigma} = 0.0331]
Data/restraints/parameters	2808/0/102	10913/0/622	3677/0/219
Goodness-of-fit on F^2	1.097	1.057	1.032
Final R indexes [I>=2σ (I)]	R_1 = 0.0271, wR_2 = 0.0676	R_1 = 0.0969, wR_2 = 0.2437	R_1 = 0.0406, wR_2 = 0.1070
Final R indexes [all data]	R_1 = 0.0298, wR_2 = 0.0690	R_1 = 0.1281, wR_2 = 0.2660	R_1 = 0.0431, wR_2 = 0.1093
Largest diff. peak/hole / e Å^{-3}	0.49/-0.22	1.29/-1.18	0.40/-0.58

11. References

1. Buchard, A.; Kember, M. R.; Sandeman, K. G.; Williams, C. K., *Chem. Comm.* **2011,** *47* (1), 212-214.
2. Wu, G.-P.; Wei, S.-H.; Ren, W.-M.; Lu, X.-B.; Xu, T.-Q.; Darensbourg, D. J., *J. Am. Chem. Soc.* **2011,** *133* (38), 15191-15199.
3. Garden, J. A.; Saini, P. K.; Williams, C. K., *J. Am. Chem. Soc.* **2015,** *137* (48), 15078-15081.
4. Della Monica, F.; Maity, B.; Pehl, T.; Buonerba, A.; De Nisi, A.; Monari, M.; Grassi, A.; Rieger, B.; Cavallo, L.; Capacchione, C., *ACS Catalysis* **2018,** *8* (8), 6882-6893.
5. Della Monica, F.; Vummaleti, S. V. C.; Buonerba, A.; Nisi, A. D.; Monari, M.; Milione, S.; Grassi, A.; Cavallo, L.; Capacchione, C., *Adv. Synth. Cat.* **2016,** *358* (20), 3231-3243.
6. Alhashmialameer, D.; Collins, J.; Hattenhauer, K.; Kerton, F. M., *Cat. Sci. Technol.* **2016,** *6* (14), 5364-5373.
7. Dengler, J. E.; Lehenmeier, M. W.; Klaus, S.; Anderson, C. E.; Herdtweck, E.; Rieger, B., *Eur. J. Inorg. Chem.* **2011,** *2011* (3), 336-343.
8. Buonerba, A.; De Nisi, A.; Grassi, A.; Milione, S.; Capacchione, C.; Vagin, S.; Rieger, B., *Cat. Sci. Tech.* **2015,** *5* (1), 118-123.
9. Whiteoak, C. J.; Gjoka, B.; Martin, E.; Belmonte, M. M.; Escudero-Adán, E. C.; Zonta, C.; Licini, G.; Kleij, A. W., *Inorg. Chem.* **2012,** *51* (20), 10639-10649.
10. Whiteoak, C. J.; Martin, E.; Belmonte, M. M.; Benet-Buchholz, J.; Kleij, A. W., *Adv. Synth. Catal.* **2012,** *354* (2-3), 469-476.
11. Fuchs, M. A.; Zevaco, T. A.; Ember, E.; Walter, O.; Held, I.; Dinjus, E.; Doring, M., *Dalton Trans.* **2013,** *42* (15), 5322-5329.
12. Sheng, X.; Qiao, L.; Qin, Y.; Wang, X.; Wang, F., *Polyhedron* **2014,** *74*, 129-133.
13. Whiteoak, C. J.; Martin, E.; Escudero-Adán, E.; Kleij, A. W., *Adv. Synth. Catal.* **2013,** *355* (11-12), 2233-2239.
14. Tamao, K.; Hayashi, T.; Ito, Y.; Shiro, M., *Organometallics* **1992,** *11* (6), 2099-2114.